



IAU-ARAK

3D-QSAR and docking analysis on a series of multi-cyclin-dependent kinase inhibitors using CoMFA, and CoMSIA

Jahan B. Ghasemi *, Mahnaz Ayati, Somayeh Pirhadi, Reihaneh Safavi-Sohi

Chemistry Department, Faculty of Sciences, K. N. Toosi University of Technology, Tehran, Iran

Received 4 April 2011; received in revised form 26 May 2011; accepted 8 June 2011

Abstract

A series of 42 Pyrazolo[4,3-h]quinazoline-3-carboxamides as multi-cyclin-dependent kinase inhibitors regarded as promising antitumor agents to complement the existing therapies, was subjected to a three-dimensional quantitative activity relationship (3D QSAR). Different QSAR methods, comparative molecular field analysis (CoMFA), CoMFA region focusing, and comparative molecular similarity indices analysis (CoMSIA), were compared. All these QSAR-based models had good statistical parameters and yielded q^2 values of 0.717, 0.806, and 0.557, respectively. The CoMFA region focusing model provided the highest q^2 and r^2 values, which implied the significance of correlation of steric and electrostatic fields with biological activities. The quality of CoMSIA was slightly lower than that of CoMFA region focusing in terms of q^2 and r^2 values. The results of 3D contour maps can be useful for the future development of CDKs inhibitors. The results of 3D QSAR models are in agreement with docking results, and the statistical parameters of the models explain that the data are well fitted and have high predictive ability.

Keywords: CoMFA; CoMFA region focusing; CoMSIA; CDOCKER; multi-cyclin-dependent kinase Inhibitors.

1. Introduction

Cancer is the leading cause of death around the world. WHO (World Health Organization) estimates that 84 million people will die of cancer from 2005 to 2015 without intervention [1]. Uncontrolled cell proliferation is the symptom of cancer, and tumor cells have typically acquired damage to genes that directly regulate their cell cycles. The cyclin-dependent kinases (CDKs) are the machines that run the cell cycle program [2-9]. The cyclin-dependent kinases such as CDK1, CDK2, CDK4, and CDK6 belong to a group of protein kinases [10]; have an important role in cell cycle regulation. Small molecules which specifically inhibit CDKs by interaction with the ATP [11] binding site are potentially valuable biochemical tools in such studies and may also have major applications as pharmaceutical agents. CDKs are also involved in the regulation of transcription and mRNA processing. A cyclin-dependent kinase is activated by association with a cyclin (Cy), while is forming a cyclin-dependent kinase complex. The

* Corresponding author.

E-mail address: jahan.ghasemi@gmail.com (J. Ghasemi).

development of agents which are able to modulate CDKs activity may have a strong effect on the prevention and therapy of cancer. G. Traquandi and co-workers recently reported a series of pyrazolo[4, 3-h]quinazoline- 3-carboxamides as CDK inhibitors. Compounds targeting complexes between cyclin-dependent kinases (CDKs) and cyclins and inhibiting their activity, are regarded as promising antitumor agents to complement the existing therapies [12].

Traditional QSAR models are insufficient to explain complex structure-activity data, since the extreme specificity of biological activity is described by three dimensional (3D) intramolecular forces and predicted on 3D molecular structures [13]. Comparative molecular field analysis (CoMFA) [14] is a powerful tool in rational drug design and related applications. CoMFA computes the steric and electrostatic fields surrounding a set of compounds and constructs a 3D QSAR model by correlating these 3D steric and electrostatic fields with the corresponding observed activities. A similar approach to the computation of molecular potential fields has been described as the comparative molecular similarity indices analysis (CoMSIA) [15], in which a probe atom is used to calculate similarity indices, at regularly spaced grid points, for the pre-aligned molecules. CoMSIA differs from CoMFA primarily in the way that the molecular fields are calculated. CoMSIA uses Gaussian-based similarity functions for molecular field calculations, while force field like potentials (e.g., Lennard-Jones and Coulomb) is predominantly used in CoMFA [14, 15]. Both 3D QSAR methods give contour maps as output that can be used to get some general insights in to the topological features of the binary sites. In computational drug design, docking tools apply to gain key structural features of binding of an inhibitor into the receptor and predicting bioactive conformers.

In the present study, the 3D QSAR studies of 42 CDKs inhibitors by CoMFA and CoMSIA have been performed, and the results of 3D contour maps can be useful for the future development of CDKs inhibitors.

2. Experimental

2.1. Materials and methods

2.1.1. Database and Computer modeling

All used compounds were reported recently by G. Traquandi and co-workers [12] as multi-cyclin-dependent kinase inhibitors. The IC_{50} (μM) values were taken in molar range and converted to pIC_{50} . The selection of suitable training set is critical for the quality of 3D QSAR models. To ensure the statistic relevance of the calculated model, the training set should contain a set of diverse compounds and their activities. So for dividing dataset to training and test sets, we have sorted the compounds according to increasing order of their biological activities. The compounds of training and test sets were selected by considering the fact that test set compounds represent a range of biological activities and chemical classes similar to training set compounds. By considering of these points, the 35 compounds were selected as training and the 7 rest compounds left out for the test set. Five compounds detected as outliers and do not consider in the model building. The structures of both the training and test set molecules are shown in Table 1. This data set used to construct 3D QSAR (CoMFA and CoMSIA) models to analysis their physico-chemical properties. Three-dimensional structures building and all pre-modeling and modeling procedures were performed by using the SYBYL 7.3 (Tripos, Inc., St. Louis, MO) running on a Red Hat Linux workstation 4.7. Gasteiger-Hückel partial atomic charges [16] and Powell's conjugate gradient method were used for minimization of all molecules with 0.01 kcal/mol Å energy gradient convergence criterion. The rest of the molecules were built by changing required substitutions on the best docked conformation of compound 12 and were energy minimized with the stated previous parameters. These molecules were then used to construct 3D QSAR (CoMFA and CoMSIA) models.

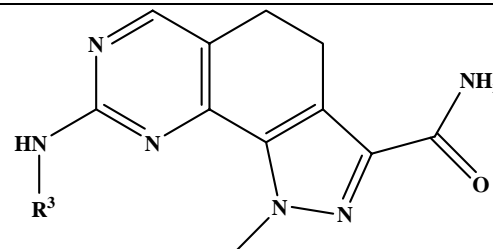
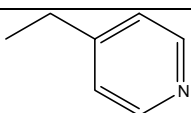
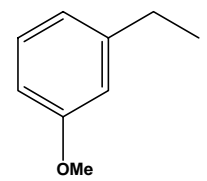
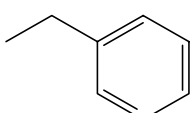
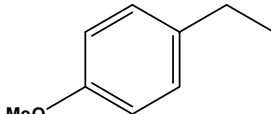
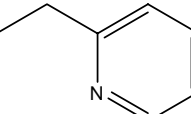
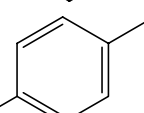
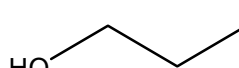
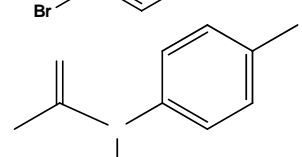
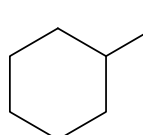
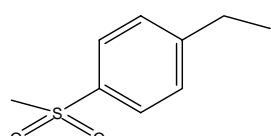
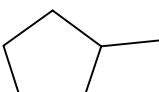
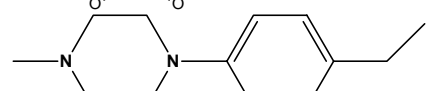
Table 1
Structures of training and test set compounds.

Comp.	R ³	R ¹	pIC ₅₀	Comp.	R ³	R ¹	pIC ₅₀
k1		NHMe	7.409	k8		NH ₂	7.921
k2		NH ₂	6.455	k9		NH ₂	9.000
k3		NHMe	5.339	k10		NHMe	7.237
k4*		NH ₂	8.699	k11		NH ₂	9.000
k5		NHMe	7.495	k12		NHMe	8.699
k6		NH ₂	8.522	k13		NH ₂	8.398
k7		NHMe	7.602	k14		NHMe	8.301

Continue Table 1

Comp.	R ²	R ¹	pIC ₅₀	Comp.	R ²	R ¹	pIC ₅₀
k15	Me	NHMe	7.013	k23		NH ₂	8.222
k16	Me		5.755	k24		NH ₂	8.301
k17*	Me		6.757	k25		NH ₂	7.000
k18	Me		6.529	k26		NH ₂	8.301
k19	Me		5.863	k27		NH ₂	8.222
k20	PhCH ₂	NH ₂	7.638	k28		NHMe	8.222
k21	Ph	NH ₂	6.699	k29*		NH ₂	8.155
k22		NH ₂	7.284				

Continue Table 1

					
	R ³	pIC ₅₀		R ³	pIC ₅₀
k30	PhCH ₂	7.292	k37		7.678
k31		7.181	k38		7.678
k32*		7.237	k39*		7.061
k33*		7.092	k40		7.721
k34		7.886	k41*		8.398
k35		7.420	k42		8.599
k36		6.983			

2.1.2. Alignment rule

Structural alignment is one of the most sensitive parameters in 3D QSAR analyses. The accuracy of the prediction of CoMFA and CoMSIA models and the reliability of the contour maps depend strongly on the structural alignment of the molecules. Best docked conformation of molecule 12 was used as the template for alignment of all the molecules in the series, assuming that its conformation represents the bioactive conformation at receptor active site level and rest of the molecules were aligned on it. The common fragment produced by Distill in SYBYL 7.3 was shown in Fig. 1 was selected for rigid automatic alignment. Aligned compounds of training set are displayed in Fig. 2.

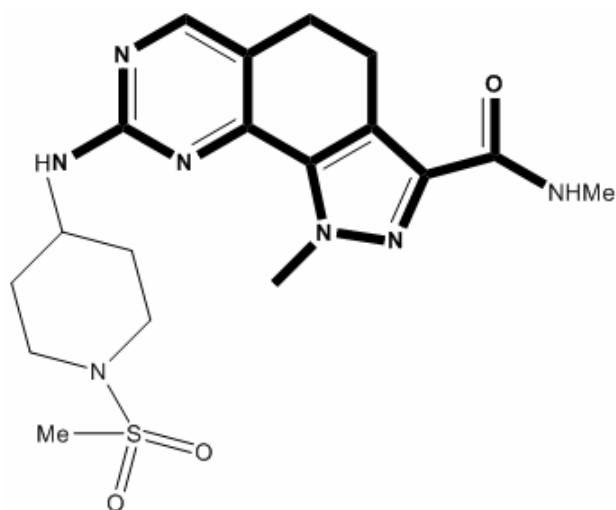


Fig. 1. Compound 12, common substructure is bolder.

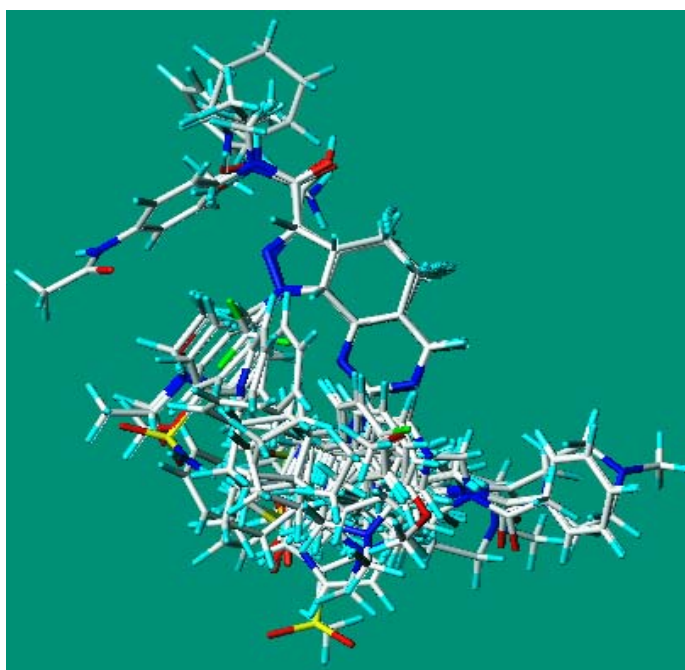


Fig. 2. Aligned training set compounds based on compound 12.

2.1.3. CoMFA and CoMSIA analysis

Following alignment, the molecules are placed one by one into a cubic lattice with various grid spacing. The steric (vdW interaction) and electrostatic (Coulombic values with a $1/r$ distance-dependent dielectric function) fields are calculated at each grid point using a sp^3 hybridized carbon probe with a +1.0 charge. The computed field energies were truncated to 30 kcal/mol for both steric and electrostatic fields. In order to reduce noise and improve efficiency, effect of different column filtering values on the CoMFA, was checked. CoMFA standard scaling, applies the equal weight to data from each lattice point in any given field. Region focusing is an iterative procedure which refines a model by improving the weight for those lattice points which are most related to the model. This enhances the resolution and predictive capability (q^2 ; cross validated r^2) of a followed PLS analysis. Technically, this corresponds to rotate the model components during a high-order space. CoMSIA is a technique in which similarity indices are calculated at different points on a regularly spaced grid for pre-aligned

molecules using a C+1 probe atom with a radius of 1.0 Å. In this approach, five different similarity fields are calculated: steric, electrostatic, hydrophobic, hydrogen bond donor and hydrogen bond acceptor. CoMSIA similarity indices $A_{F,k}^q(j)$ for a molecule j with atoms i at grid point q are calculated by Eq.1.

$$A_{F,k}^q(j) = - \sum W_{\text{probe},k} W_{ik} e^{-\alpha r_{iq}^2} \quad (1)$$

In Eq.1 A is the similarity index at grid point q , summed over all atoms i of the molecule j ; $W_{\text{probe},k}$ is the probe atom with radius 1.0 Å, charge +1, hydrophobicity +1, hydrogen bond donating +1, hydrogen bond accepting +1; W_{ik} is the actual value of the physicochemical property k of atom i ; r_{iq} is the mutual distance between the probe atom at grid point q and atom i of the test molecule. Alfa (α) is the attenuation factor, with a default value of 0.3, and an optimal value normally ranging from 0.2 to 0.4 [17-20]. A Gaussian type distance dependence function was used between the grid point q and each atom i of the molecule.

2.1.4. Docking Analysis

The crystal structure of 2WXV/CYCLIN-A2 in complex with compound 12 was taken from RCSB protein databank (<http://www.pdb.org>). Then structures of other compounds were constructed via modifying the extracted compound 12 from the receptor, in SYBYL 7.3. For docking analysis, compound 9 fed to Discovery Studio 2.5 (Accelrys Inc, San Diego, CA, USA), and was typed with CHARMM force field, and Momany-Rone partial charges were calculated [21]. The resulting structure was minimized with Smart Minimizer, performs 1000 steps of steepest descent with a RMS gradient tolerance of 3, followed by Conjugate Gradient minimization [22]. For preparation step of enzyme, the complex typed with CHARMM force field, hydrogen atoms were added, all water molecules removed, and pH of protein adjusted to almost neutral, 7.4, using protein preparation protocol. The inhibitor was again minimized in-situ with Smart Minimizer option that is custom for in-situ ligand minimization and consists of some pre-defined minimization steps that have been pre-determined to work well for receptor ligand data [22]. An 8.8 Å radius sphere defined around the bounded ligand (compound 12) to confirm some residues are free to move. Then bounded inhibitor removed from the binding site. Other parameters were established by default protocol settings. CDOCKER, (CHARMM-based DOCKER) and a molecular dynamics (MD) simulated-annealing based algorithm, used to dock inhibitor 9 into the receptor. CDOCKER is an implementation of a CHARMM based docking tool using a rigid receptor that generates several prime random ligand orientations within the receptor active site followed by MD-based simulated annealing, and final refinement by minimization. During the docking, van der Waals (vdW) and electrostatics (non-bonded interactions) are softened at different levels, but this softening is deleted for the ultimate minimization [23]. For each final conformation, the CDOCKER score accounted as the negative value (interaction energy plus ligand strain) and employed to rank the poses of every input ligand [23].

2.1.5. Regression analysis

To drive 3D QSAR models, the CoMFA and CoMSIA descriptors were used as independent variables and the pIC_{50} values as dependent variables. A partial least-squares (PLS) methodology [24, 25], which is an extension of multiple regression analysis, was conducted with the standard implementation in the SYBYL 7.3 package. The predicted values of the models were first evaluated by Leave-One-Out cross validation and the cross validated coefficient (q^2) was calculated using Eq.2.

$$q^2 = 1 - \frac{\sum_{i=1}^n (Y_{\text{observed}} - Y_{\text{predicted}})^2}{\sum_{i=1}^n (Y_{\text{observed}} - Y_{\text{mean}})^2} \quad (2)$$

Where y_i is the activity for training set compounds, y_m is the mean observed value corresponding to the mean of the values for each cross validation group, and $y_{\text{Pred},i}$ is the predicted activity for y_i . To validate the derived CoMFA and CoMSIA models, biological activity of an external test set of seven compounds were predicted using models derived from the training set. The predictive r^2 (r^2_{pred}) value was calculated using Eq. 3

$$r^2_{\text{pred}} = \frac{SD - \text{PRESS}}{SD} \quad (3)$$

where SD is the sum of squared deviations between the biological activity of the test set and the mean activity of training set molecules, and PRESS is the sum of squared deviation between the actual and the predicted activities of the test set.

3. Result and Discussion

The idea underlying the CoMFA methodology is that differences in biological activity are often related to difference the magnitudes of molecular fields surrounding the receptor ligand investigated. The high value of LOO q^2 appears to be the necessary but not the sufficient condition for the model to have a high predictive power; this is the general property of QSAR models developed using LOO cross-validation, really the external validation is the only way to establish a reliable QSAR model [26]. To investigate the robustness and predictive ability of 3D QSAR models, cutoff, grid spacing, and column filtering values were changed to reach the best models.

3.1. CoMFA and CoMFA region focusing

The best results were obtained at a column filtering of 2 kcal/mol, grid spacing 1 Å, and cutoff value of 20 kcal mol⁻¹ for both steric and electrostatic fields. The results of CoMFA studies based on changing cutoff values are summarized in Table 2. The optimal number of components was determined by selecting highest q^2 value, which corresponds to lowest S_{press} value. PLS analysis showed a high q^2 value of 0.717 with six components for CoMFA. The non cross-validated PLS analysis results in a conventional r^2 of 0.965, $F = 129.857$, and a standard error of estimation (SEE) of 0.188. To assess the statistical confidence limits of the derived models, bootstrapping analysis was carried out with 100 runs. Bootstrapping involves the generation of many new datasets from the original datasets after randomly choosing samples from the original dataset that r^2_{bs} was obtained 0.981. The test set was used to further verify the constructed model that r^2_{pred} was obtained 0.767. After focusing these fields, the q^2 improved and produced highest q^2 of 0.806 at column filtering 3 kcal/mol with six components, $F = 101.001$, $r^2_{\text{ncv}} = 0.956$, a standard error of estimation of 0.205, $r^2_{\text{bs}} = 0.970$, and r^2_{pred} for test set = 0.813. Steric field descriptors explain 0.916 of the variance, while the electrostatic descriptors explain 0.084. This shows important effect of steric fields in biological activity. Results for CoMFA region focusing are shown in Table 3, and the correlation between the predicted activities and the experimental activities are depicted in Fig. 3. The CoMFA steric and electrostatic fields from the final best non-cross-validated analysis were plotted as 3D colored contour maps. The field energies at each lattice point were calculated as the scalar results of the coefficient and the standard deviation associated with a particular column of the data table (SD*coeff), as always plotted as the percentages of the contribution of CoMFA equation. These maps show regions where differences intermolecular fields are associated with differences in biological activity in

terms of steric (80% green, 20% yellow) and electrostatic (80% blue and 20% red). Greater values of bio-activity are correlated with more bulk near green, less bulk near yellow, more positive charge near blue and more negative charge near red. The contours for CoMFA steric and electrostatic fields are displayed in Fig. 4a and b respectively. CoMFA contour maps show green in R^3 , suggest that a more sterically bulky is favorable and increase the activity, which may explain why compounds 4-9, and 11-14 are more potent than compound 1 and compound 3. Also presence of green regions near phenyl substituents in R^3 (in compounds 34 and 30) indicate that why activity of compound 34 is higher than compound 30. The yellow regions near R^1 position explain less bulky groups would increase the activity. It can explain the fact that the activity of compounds 20, and 20-29 is more than compounds 16-19. In addition the activity of compounds having amino group in R^1 position is higher than that of the corresponding compounds having aminomethyl at that position: $2 > 3$, $4 > 5$, $6 > 7$, $9 > 10$, $11 > 12$, $13 > 14$. The presence of the blue region besides R^2 position indicate more positive groups increase the activity, and explain why activity of compound 27 with a more electropositive substituent at that position is higher than compound 29. The presence of a red contour near the carbonyl group of compounds 5-8 indicates that increase in electronegativity nature at this position can be useful for the activity.

Table 2

Statistical parameters of CoMFA with grid spacing of 1 and columnfiltering of 2, in different cutoff values.

Statistical parameters *	Cutoff value (kcal/mol)					
	10	20	30	40	50	60
q^2	0.679	0.717	0.639	0.575	0.577	0.598
r_{ncv}^2	0.951	0.965	0.963	0.960	0.964	0.966
r_{bs}^2	0.965	0.981	0.974	0.983	0.978	0.979
F	90.060	129.857	22.459	111.422	124.944	131.314
SEE	0.216	0.188	0.187	0.195	0.185	0.180
S	0.77	0.775	0.780	0.762	0.740	0.734
E	0.229	0.225	0.220	0.238	0.260	0.266

Table 3

Statistical parameters of CoMFA region focusing model with grid spacing of 1 and cutoff value of 20.

statistical parameters *	Column filtering					
	0.5	1	1.5	2	2.5	3
q^2	0.728	0.728	0.729	0.728	0.742	0.806
r_{ncv}^2	0.963	0.963	0.962	0.955	0.953	0.956
r_{bs}^2	0.979	0.979	0.979	0.977	0.974	0.970
F	122.28	122.128	119.308	99.197	94.096	101.001
SEE	0.187	0.187	0.189	0.207	0.212	0.205
S	0.770	0.77	0.772	0.778	0.832	0.916
E	0.230	0.233	0.228	0.222	0.168	0.084

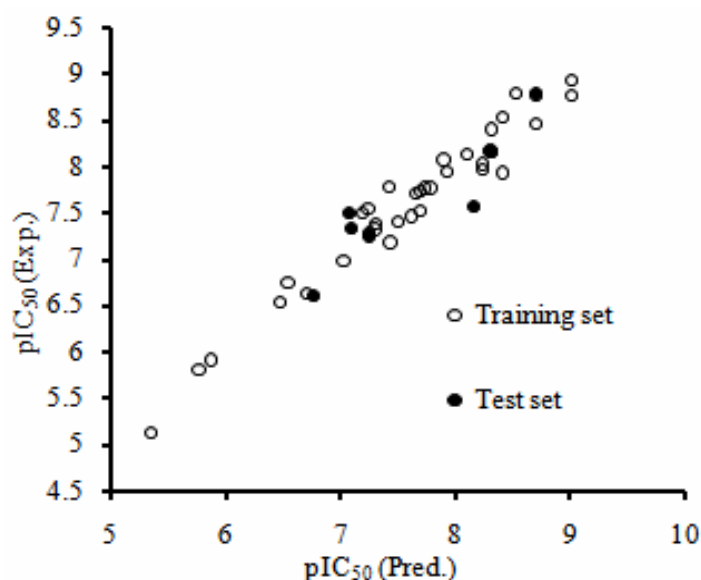


Fig. 3. Plot of experimental against predicted activities for the training and test set compounds based on the best CoMFA region focusing model.

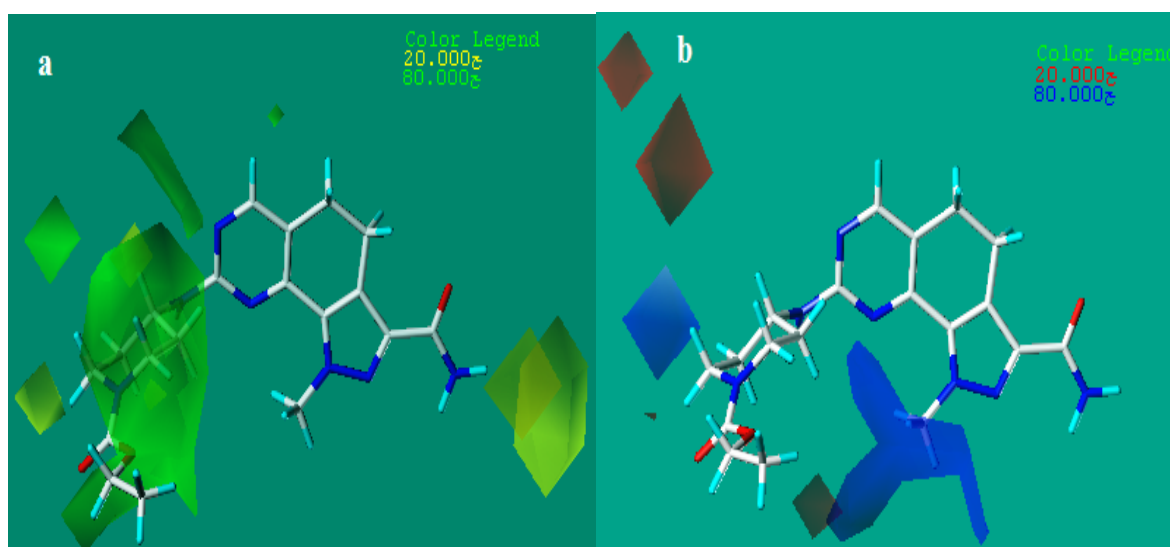


Fig. 4. Contour maps of CoMFA based on compound 9: steric (a), and electrostatic (b).

3.2. CoMSIA study

The CoMSIA analysis was done at a grid spacing of 1 Å, and the effect of column filtering was tested with the combination of five fields. The CoMSIA method defines explicit hydrophobic (H), hydrogen bond donor (D), and hydrogen bond acceptor (A) descriptors in addition to the steric (S) and electrostatic (E) fields in CoMFA. To select the optimal result, we systematically changed the combination of fields. Fig. 5 shows the distribution of q^2 that resulted from the different field combinations. The highest q^2 of 0.557 was obtained with six components at a column filtering of 2 kcal/mol, grid spacing of 1 Å, $F = 159.879$, non-cross-validated r^2 of 0.972, $SEE = 0.164$, and $r^2_{bs} = 0.986$ for the steric, electrostatic, and hydrogen bond donor fields. The corresponding field contributions of steric, electrostatic, and hydrogen bond donor are 0.304, 0.326, and 0.370 respectively. The correlation between the predicted activities and the experimental activities are depicted in Fig. 6. Figs. 7a, b and c are corresponding to the best model (steric, electrostatic, and hydrogen bond donor) of CoMSIA. The steric and electrostatic

contour maps are nearly similar to that of CoMFA. In steric contour maps, greater values of bioactivity are correlated with more bulk near green and less bulk near yellow, in electrostatic contour maps more positive charge near blue and more negative charge near red increase the activity. In hydrogen bond donating contour maps, cyan contours indicate regions where hydrogen bond donor groups increase activity; purple contours represent regions where hydrogen bond donor groups decrease activity. There is a cyan region near R^1 indicate the activity of compounds having amino group at R^1 position is higher than that of the corresponding compounds having aminomethyl at that position: $2 > 3$, $4 > 5$, $6 > 7$, $9 > 10$, $11 > 12$, $13 > 14$. There are two big purple contour maps in the Fig. 7c, surrounding the R^3 position on the heterocyclic ring, indicate that any hydrogen bond acceptor groups are not favored in these areas. R^3 region is important due to the presence of red and purple (in CoMSIA contour maps), and green polyhydra in both of CoMSIA and CoMFA contour plots. It can be stated that the most predominate interactions between ligand and receptor binding sites (aminoacid residues), according to docked conformer of molecule 9 and the results of the CoMFA and CoMSIA modeling, are hydrogen bonding, ionic interaction or salt bridge, electrostatic and hydrophobic interaction.

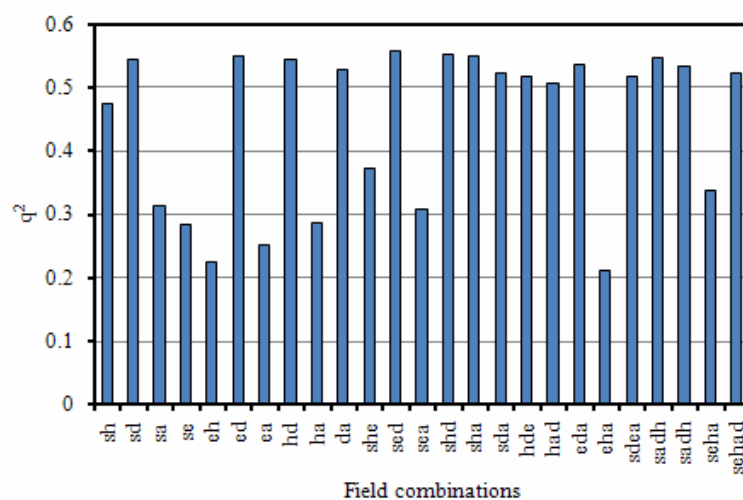


Fig. 5. Cross-validated r^2 (q^2) for different field combinations.

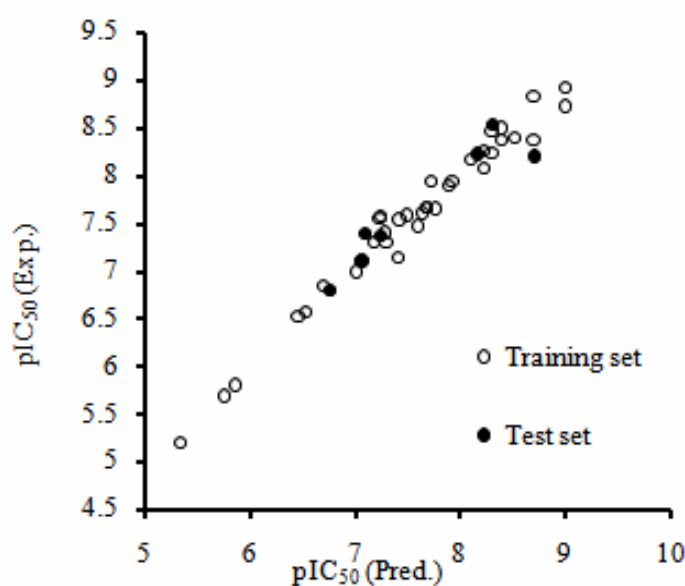


Fig. 6. Plot of experimental against predicted activities for the training and test set compounds based on the best CoMSIA model.

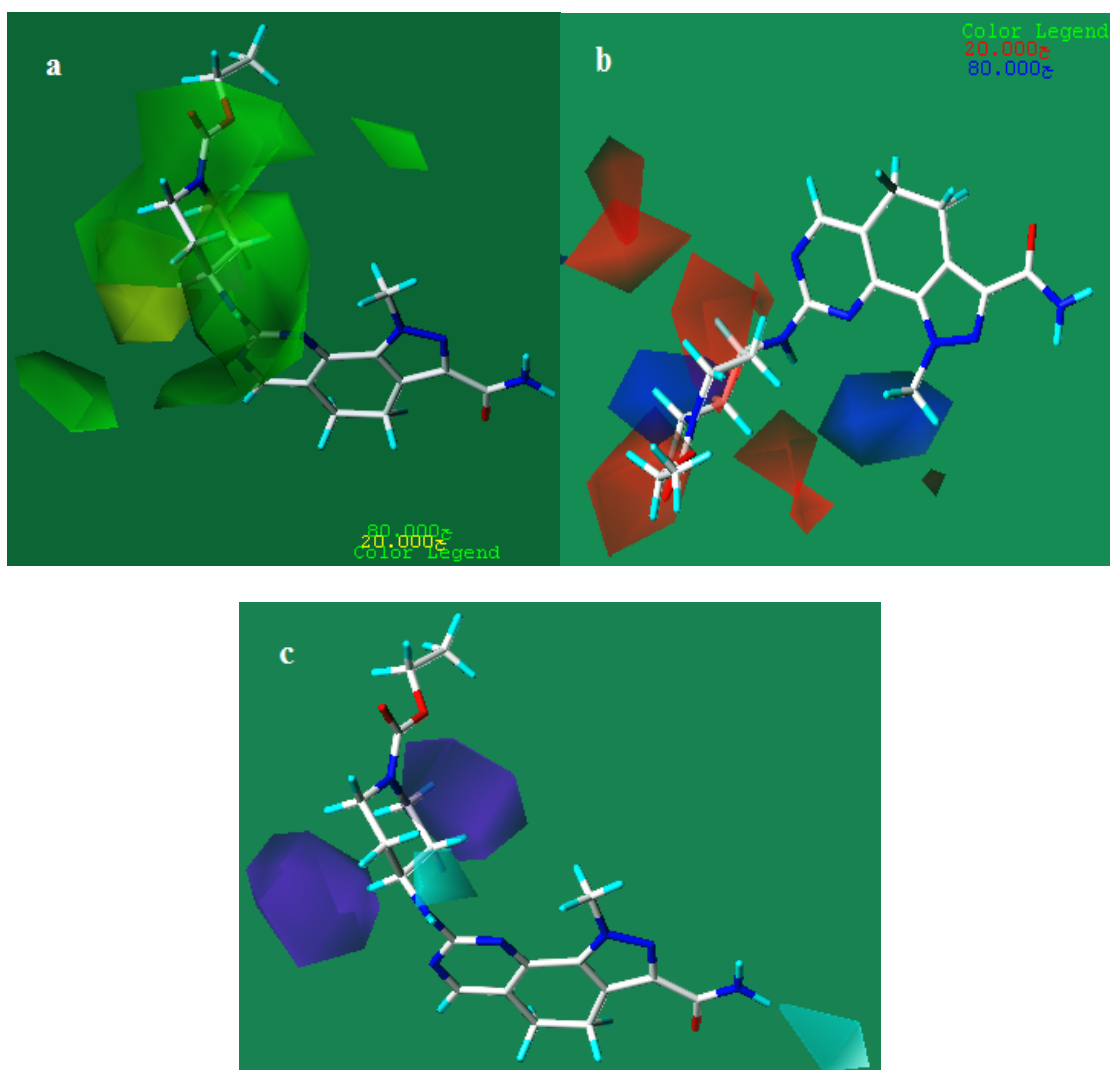


Fig. 7. CoMSIA contour maps based on compound 9: steric (a), electrostatic (b), and hydrogen bond donor fields (c).

3.3. Docking interpretation

In our docking studies, it was observed that these compounds interact with the CDK2/Cyclin-A2 active site through an extensive hydrogen bond network, including mainly the following residues: Leu83, Lys32, Asp86 and Tyr15 (Fig. 8). Therefore, in order to understand the importance of such interactions in the series of pyrazolo[4,3-h]quinazoline-3-carboxamide as CDK2 inhibitors, it was performed a correlation between the compounds (substituents) hydrogen bond donor ability and the compound potency. The contour plot of the cyan polyhedrons (contribution level of 80%) close to NH_2 of carboxamide group and $-\text{NH}$ connected to dihydroquinazoline group in compound 9 (Figure 7c) indicates active site favorable regions in order to group interact with hydrogen bond donor ability group, since substituents such as $-\text{OH}$ and $-\text{NH}$ groups in these position increase the inhibitory potency. Also presence of electrostatic blue contour near the NH_2 of carboxamide group confirm the cyan contour, because H atom of the NH at this position has the positive charge because of its hydrogen bonding nature. Complementary of this cyan contour in the receptor, are hydrogen bond acceptor residues Leu83 and Tyr15 in CDK2 active site. Carbonyl group and O in carboxylic group in compound 9 form hydrogen bonds with Lys89 and Asp86, respectively, and carbonyl in carboxamide group and N

in dihydroquinazoline acted as a hydrogen bond acceptor by binding to the NH₂ and NH groups in Lys33 and Leu83, respectively.

A yellow contour is around NH₂ of carboxamide group, indicates that a less bulky group would be favorable: more bulky groups such as NHMe because of probable steric clashes with Tyr15, Val18, Lys33, and Asp145 would decrease the activity, and a green contour near R³ explains a more bulky group increase activity, because these substitutions optimally fill the hydrophobic part of binding site.

The MOLCAD molecular surface of the ATP-binding site were developed and then displayed with hydrogen bonding, lipophilic and electrostatic potential to examine the hydrophobic, hydrogen bond contour maps and the electrostatic contour maps. In Fig. 9a, the red color shows the electron-withdrawing zone and purple color shows electron donating zone. The R¹ position of compound 9 was found in the red area. Compound 9 is into an electropositive blue area that confirm electrostatic contour map in Fig.7b. In Fig.9b, The brown color represents highest lipophilic area of the molecule while blue indicates hydrophilic region, the R² position of compound 9 was found in the hydrophobic blue area. In Fig.9c, the red represent highest hydrogen bond donating and blue color displays highest hydrogen acceptor area. According to this figure, hydrogen bond donor groups (such as NH and NH₂) are in corresponding to blue regions, and hydrogen bond acceptor (O and N) with red regions.

In this study, the bioactive conformation of molecule 12 was used as template for alignment, and then the QSAR methods CoMFA, and CoMSIA, were used to investigate the relationship between the structures of 35 cyclin-dependent kinases inhibitors and their activities, by using the Distill alignment routine in SYBYL 7.3. The high q^2 and r^2_{pred} values obtained from these different QSAR methods suggest that we successfully acquired QSAR models. The effects of the steric, electrostatic, and hydrogen bond donor fields around the aligned molecules on their activities were clarified by analyzing the CoMFA and CoMSIA contour maps. The information from this study suggests that incorporating steric bulk, higher degree of electronegativity on R³ substitution might be favorable for better Pyrazolo[4,3-h]quinazoline-3-carboxamides as multi-cyclin-dependent kinase Inhibitors, but presence of hydrogen bond donor groups in this position is not favored. The CoMFA region focusing model provided the most significant correlation of steric and electrostatic fields with the biological activities. It was superior over the CoMFA standard model. The q^2 values obtained from CoMSIA were slightly lower than CoMFA but CoMSIA is very fast in data processing. From these analyses, it is possible to predict the ligand activities of newly designed cyclin-dependent kinases inhibitors, and design better anti cancer inhibitors.

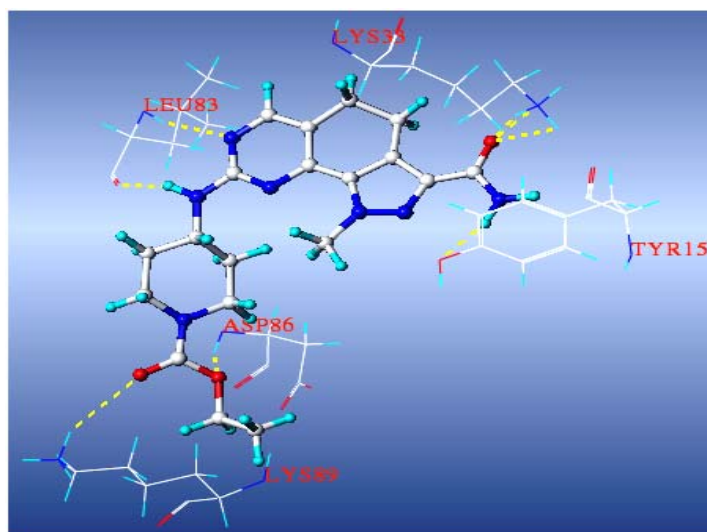


Fig. 8. A stereo view of the active site of ATP-binding site of CDK2/cyclin-A2 showing molecule 9 with important receptor residues.

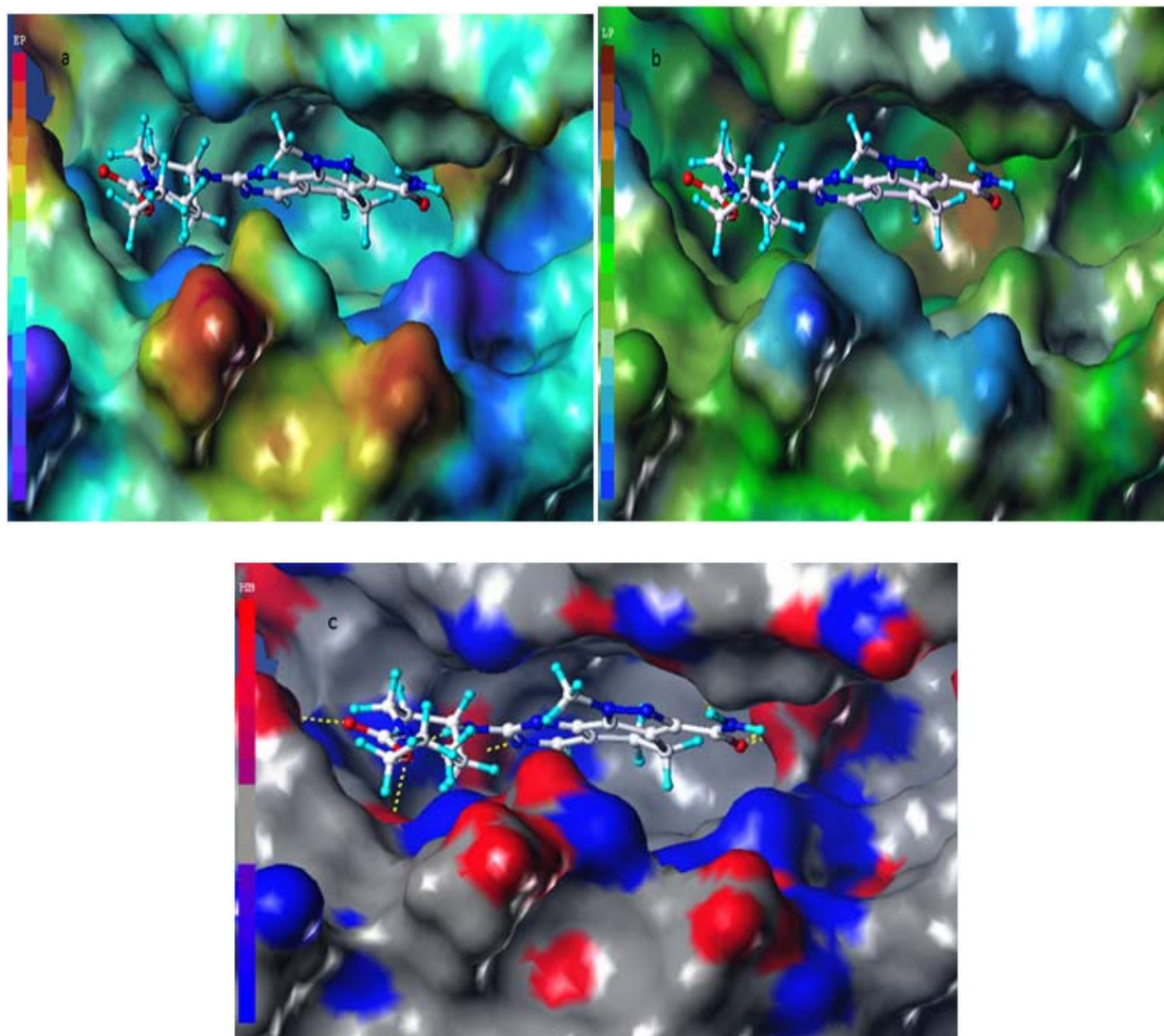


Fig. 9. The MOLCAD electrostatic (a), lipophilic (b), hydrogen bonding (c) surface of ATP-binding site of CDK2/cyclin-A2 (PDB code: 2WXV) within the compound 9.

References

- [1] http://www.who.int/mediacentre/events/annua/world_cancer_day/en.
- [2] D.O. Morgan, *Nature*, 374 (1995) 131-134.
- [3] D. Morgan, *Annu. Rev. Cell. Dev. Biol.* 13 (1997) 261-291.
- [4] Y.T. Chang, N.S. Gray, G.R. Rosania, D.P. Sutherlin, S. Kwon, T.C. Norman, R. Sarohia, M. Leost, L. Meijer, P.G. Schultz, *Chem. Biol.* 6 (1999) 361-375.
- [5] W.F. De Azevedo, S. Leclerc, L. Meijer, L. Havlicek, M. Strnad, S.H. Kim, *Eur. J. Biochem.* 243 (1997) 518-526.
- [6] P. Imbach, H.G. Capraro, P. Furet, H. Mett, T. Meyer, J. Zimmermann, *Bioorg. Med. Chem. Lett.* 9 (1999) 91-96.
- [7] R. Hoessel, S. Leclerc, J. Endicott, M. Noble, A. Lawrie, P. Tunnah, M. Leost, E. Damiens, D. Marie, D. Marko, E. Niederberger, W. Tang, G. Eisenbrand, L. Meijer, *Nat. Cell. Biol.* 1 (1999) 60-67.
- [8] C. Schultz, A. Link, M. Leost, D.W. Zaharevitz, R. Gussio, E.A. Sausville, L. Meijer, C. Kunick, *J. Med. Chem.* 42 (1999) 2909-2919.
- [9] L.L. Kent, N.E. Hull Campbell, T. Lau, J.C. Wu, S.A. Thompson, M. Nori, *Biochem. Biophys. Res. Commun.* 260 (1999) 768-774.
- [10] G. Manning, D.B. Whyte, R. Martinez, T. Hunter, S. Sudarsanam, *Science* 298 (2002) 1912-1934.

- [11] D.H.L. De Bondt, J. Rosenblatt, J. Jancarik, H.D. Jones, D.O. Morgan, S.H. Kim, *Nature* 363 (1993) 595-602.
- [12] G. Traquandi, M. Ciomei, D. Ballinari, E. Casale, N. Colombo, V. Croci, F. Fiorentini, A. Isacchi, A. Longo, C. Mercurio, A. Panzeri, W. Pastori, P. Pevarello, D. Volpi, P. Roussel, A. Vulpetti, M. Gabriella Brasca, *J. Med. Chem.* 53 (2010) 2171-2187.
- [13] R. Garg, S.P. Gupta, H. Gao, M.S. Babu, A.K. Debnath, C. Hansch, *Chem. Rev.* 99 (1999) 3525-3602.
- [14] R.D. Cramer, D.E. Patterson, J.D. Bunce, *J. Am. Chem. Soc.* 110 (1989) 5959-5967.
- [15] G. Klebe, U. Abraham, T. Mietzner, *J. Med. Chem.* 37 (1994) 4130-4146.
- [16] A. Streitwieser, *Molecular Orbital Theory for Organic Chemists*, Wiley, New York, 1961.
- [17] G. Folkers, A. Merz, D. Rognan, *3D-QSAR in Drug Design in: H. Kubinyi (ed) Theory, Methods and Applications. The Netherlands*, p. 583. ESCOM, Leiden, 1993.
- [18] V.N. Viswanadhan, A.K. Ghose, G.R. Revankar, R.K. Robins, *J. Chem. Inf. Comput. Sci.* 29 (1989) 163-172.
- [19] S. Kamath, J.K. Buolamwini, *Med. Chem.* 46 (2003) 4657-4668.
- [20] M. Bohm, J. Sturzebecher, G. Klebe, *J. Med. Chem.* 42 (1999) 458-477.
- [21] F.A. Momany, R. Rone, *J. Comput. Chem.* 13 (1992) 888-900.
- [22] *Discovery Studio. Accelrys Software Inc, San Diego, CA, 2009.*
- [23] W.U. Guosheng, D.H. Robertson, III C.L. Brooks, M. Vieth, *J. comput. chem.* 24 (2003) 1549-1562.
- [24] R.D. Cramer, J.D. Bunce, D. E. Patterson, *Quant. Struct. Act. Relat.* 7 (1988) 18-25.
- [25] P. Geladi, *J. Chemometrics*, 2 (1988) 231-246.
- [26] A. Golbraikh, A. Tropsha, *J. Mol. Graph. Model.* 20 (2002) 269-276.